GNSS meteorology and impact on NRT position

H. Brenot[1], G. Wautelet[2], R. Warnant[2], J. Neméghaire[3] and M. Van Roozendael[1]

[1] Belgian Institute for Space Aeronomy (BIRA-IASB), Belgium, brenot@oma.be
[2] University of Liège (ULg), Belgium.
[3] Royal Meteorological Institute (IRM-KMI), Belgium.

Abstract: The analysis of GNSS signal and the use a dense network of ground-based stations allow to measure tropospheric parameters that can be used for near real-time (NRT) meteorological applications (e.g. monitoring of the delay of the neutral atmosphere and the detection of blobs of water vapour). On the other hand, the meteorological activity can impact GNSS positioning solutions. For this reason, NRT indicators of the tropospheric activity related to the disturbance of GNSS signal are required. Using a dense network of GNSS stations, this study presents a new NRT indicator based on the double differences of the ionosphere-free combination. To validate this indicator, the impact of severe weather conditions on RTK positioning solutions is shown.

BIOGRAPHIES

A. Hugues Brenot has a background in Geodynamics (master Thesis about the implementation of reological model of Mars planet at EOST/University of Strasbourg, 2002), in Geodesy and GNSS meteorology (PhD at the University of Grenoble IsTerre/OSUG and Météo-France/CNRM Toulouse, 2006). Involved in GALOCAD/ESA project (2006-2008) at IRM-KMI, he is developing since 2010 the monitoring of volcanic plume using remote sensing at BIRA-IASB (http://sacs.aeronomie.be). His research still focuses on the detection of tropospheric/ionospheric signature in the GNSS signal; work achieved in the frame of the Solar-Terrestrial Centre of Excellence (STCE) and the GNSS4SWEC COST Action.

B. Gilles Wautelet has a PhD in Sciences and is a post-doctoral researcher at the Geomatics Unit (ULg) with 7 years experience in GNSS research. He previously worked in the frame of the FP6 GALOCAD project and of the SWANS project (funded by the Belgian Science Policy) to develop ionospheric products for end-user communities, like land surveyors or civil engineers. His research focuses on ionospheric disturbances and their influence on high-accuracy positioning with dual-frequency GNSS receivers. He also has an interest in ionospheric physics and statistics, in particular applied to time series analysis.

C. René Warnant started his career as a geodesist at the Royal Observatory of Belgium in 1988. His main area of research is the mitigation of ionospheric effects on GNSS. His Ph. D. was dedicated to the reconstruction of the ionosphere Total Electron Content using dual frequency GPS measurements. He has also been involved in water vapour reconstruction and ground deformation monitoring based on GNSS. In 2007, he left the Royal Observatory to become Head of Division “Ionospheric profiles” at Royal Meteorological Institute of Belgium. Since June 2011, he is full time Professor and Head of Laboratory Geodesy and GNSS at the University of Liège where he is responsible of education in the field of Space Geodesy and GNSS.

D. Jean Neméghaire is a forecasters at IRM-KMI.

E. Michel Van Roozendael is a senior scientist at BIRA-IASB, leader of the UV-Vis DOAS group. With a background in optical spectroscopy and atmospheric chemistry research, he has been developing trace gas retrieval remote-sensing applications for more than 20 years, using ground-based, satellite and aircraft platforms. Through his involvement in the successive ESA and EUMETSAT atmospheric composition missions (ERS-2 GOME, ENVISAT, METOP, Sentinels 4,5,5P) he has contributed to the development of level-2 algorithm baselines for a number of trace data products from the GOME, SCIAMACHY and GOME-2 instruments. He is member of the GOME, SCIAMACHY and OMI Science Advisory Groups, and of the Sentinel 5 Precursor Mission Advisory Group. Since 2004, he is also co-chair of the UV-Visible working group of the International Network for the Detection of Atmospheric Composition Change (NDACC). Since the early nineties, he has been involved in over 75 EU, ESA, EUMETSAT and national projects, and he has been author or co-authors of more than 120 peer-reviewed publications. He is currently Science Leader of the ESA Ozone Climate Change Initiative project and PI of the Belgian contribution to the EUMETSAT O3MSAF and the ESA Sentinel-5 Precursor mission.

1 INTRODUCTION

The disturbance of the propagation of GNSS signal through the troposphere and recorded by ground-based receivers can precisely be estimated and used as a meteorological parameter. In particular geodetic software can retrieve three tropospheric parameters. The following section gives a description of their establishments. The first indicator of tropospheric activity is the zenith total delay of the neutral atmosphere (so called ZTD). The second one is the horizontal delay gradients (based on two components NS and EW). The third tropospheric parameter is the slant delay of the neutral atmosphere in direction of GNSS satellites (so called STD). An example of these GNSS indicators of meteorological activity is presented showing the interest for nowcasting. The error in propagation of GNSS signal induced by the meteorological activity can have a direct impact on GNSS positioning solutions. The section 3 of this paper introduces a new near real-time (NRT) indicator of meteorological activity based on double-difference of the ionosphere-free combination (so called IF DD Index). To validate the interest of this meteorological indicator for NRT positions, the related impact on real-time kinematic (RTK) position is shown in section 4. Finally, we conclude about future works. The present work has been initiated in the frame GALOCAD/ESA project (GAlileo LOcal Component for nowcasting and forecasting Atmospheric Disturbances, 2006-2008).

2 GNSS METEOROLOGICAL PRODUCTS

2.1 The zenith total delay of the neutral atmosphere

The neutral atmosphere affects the propagation of electromagnetic waves. In particular, it introduces a delay in the propagation of GNSS microwave signals. This delay essentially due to the troposphere and the low stratosphere is commonly called “tropospheric delay”. The GNSS satellites transmit two signals at frequencies L_1 (1575.42 MHz) and L_2 (1227.6 MHz). Neglecting multipath effects, the simplified mathematical model of phase measurements (φ_A^i) made by receiver *A* on satellite *i* can be considered (*Seeber*, 2003; *Leick*, 2004):

$$\varphi_A^i = \frac{f}{c}\left(D_A^i + T_A^i - I_A^i + c\left(\Delta t^i - \Delta t_A\right)\right) + N_A^i \qquad (1)$$

This model depends on the geometric distance between receiver *A* and satellite *i* (D_A^i), the ionospheric error (I_A^i), the tropospheric error (T_A^i), the receiver clock synchronisation error (Δt_A), the satellite clock synchronisation error (Δt^i), the phase ambiguity (integer number N_A^i),, the considered carrier frequency f (L_1 or L_2), and the speed of electromagnetic waves (*c)*.

The tropospheric error (T_A^i) is the path delay of the neutral atmosphere (so called the tropospheric path delay). It can be defined by three contributions:

$$T_A^i = T_{hydrostatic}{}_A^i + T_{wet}{}_A^i + T_{hydrometeors}{}_A^i \qquad (2)$$

The tropospheric path delay (T_A^i) is essentially induced by the thickness and the density of the neutral atmosphere. This major contribution (generally about 90% of T_A^i at the sea level in Belgium) which depends on the altitude and on the absolute pressure of the station, is called the *“hydrostatic delay”* ($T_{hydrostatic}{}_A^i$); see *Saastamoinen* (1972). Another contribution to T_A^i takes place at GNSS frequencies. In fact, the molecule of water vapour owns a dipolar moment that induces a delay effect on microwave propagation. This second contribution is called the *“wet delay”* ($T_{wet}{}_A^i$); see *Saastamoinen* (1972). The variability of the tropospheric error (T_A^i) is principally controlled by the water vapour density through the atmospheric path travel (from 2% to 20% of T_A^i at the sea level). A third contribution to the tropospheric error exits: this is the

contribution of hydrometeors ($T_{hydrometeors_A}^{i}$) to the total delay of the neutral atmosphere (*Solheim et al.*, 1999; *Hajj et al.*, 2001; *Brenot et al.*, 2006). This small contribution to tropospheric path delay owns a relative high variability (from 0% to 3% of T_A^i).

The tropospheric error (T_A^i) can be converted to a zenith tropospheric error above a GNSS station *A*. Taking into account the variable composition and thickness of the neutral atmosphere in the direction of a satellite *i* (at azimuth α_i and elevation ε_i) visible from station *A* at time *t*, an approximation of the vertical tropospheric error ($T_A^{vertical}$) can be estimated using mapping function (*MF*):

$$T_A^i(t) \cong T_A^{vertical}(t) . MF(t, \alpha_i, \varepsilon_i) \quad (3)$$

If the atmosphere were rigorously plan without local tropospheric anisotropy around station *A*, the simple mapping function (without azimuth dependency) is $sin^{-1}(\varepsilon_i)$. Nevertheless in practice, for low elevations this simple function is generally not realistic (*Resch*, 1984; *Bevis et al.*, 1992). More complicated mapping functions have thus been introduced to convert more precisely slant delays into zenith delays taking into account the more important thickness of the troposphere at low elevation and the error caused by the straight line approximation (*Hopfield*, 1969; *Marini and Murray*, 1973; *Ifadis*, 1986; *Herring*, 1992; *Niell*, 1996; Boehm et al., 2006).

In the literature, the term $T_A^{vertical}$ (Eq. 3) is often referred to as the *"Zenith Total Delay"* of the neutral atmosphere (ZTD). The ZTD expresses the mean zenith additional distance travels by GNSS signal through the empty space comparing to the propagation through the neutral atmosphere for the same time of travel (ZTD values are about 2.5 m at the sea level):

$$ZTD = ZHD + ZWD + ZHmD \quad (4)$$

The major part of the ZTD depends on the altitude and the absolute pressure at the station. This major contribution is called the "*Zenith Hydrostatic Delay*" (ZHD), and is about 2.3 m at the sea level. On the other hand, the major variation of ZTD is essentially driven by the water vapour content over the site: the "*Zenith Wet Delay*" contribution (ZWD) ranges from 0.05 m to 0.50 m. *Brenot et al.* (2006) have shown that an additional contribution to ZTD can be considered during rainfall event: the "*Zenith Hydrometeors Delay*" (ZHmD) with value estimate up to 0.07 m during the flash-flood event which occurred the 8-9 September 2002 over southeastern France.

In term of meteorological application, geodetic software can allow the adjustment of ZTD (sub-hourly process, see Haan et al., 2006). To extract the tropospheric error (T_A^i) from the phase measurements (φ_A^i) four steps have to be considered:

Step 1: the Ionosphere-Free combination

Contrary to the ionosphere, the troposphere is non-dispersive for GNSS microwaves. Thus, the Ionosphere-Free (IF) combination allows to remove the first order of ionospheric errors. Considering the simplified mathematical model of phase measurements φ presented Eq. 1, and according to φ_1 and φ_2, respectively the phase measurements at L_1 and L_2 frequencies, the IF combination is given by:

$$\varphi_{IF} = \alpha_{IF}\, \varphi_1 + \gamma_{IF}\, \varphi_2 \quad (5)$$

with

$$\alpha_{IF} = \frac{{f_1}^2}{\left({f_1}^2 - {f_2}^2\right)} \cong 2.546 \quad (6)$$

and

$$\gamma_{IF} = -\frac{f_1 f_2}{\left(f_1^2 - f_2^2\right)} \cong -1.984 \quad (7)$$

If we neglect multipath, the IF phase measurements $\varphi^i_{A,IF}$ made by receiver *A* on satellite *i* can be expressed by:

$$\varphi^i_{A,IF} = \frac{f_1}{c}\left(D^i_A + T^i_A\right) + f_1\left(\Delta t^i - \Delta t_A\right) + N^i_{A,IF} \quad (8)$$

where f_1 is the frequency of L_1, and $N^i_{A,IF}$ the phase ambiguity of the IF combination (real number) which can be formulated by:

$$N^i_{A,IF} = \alpha_{IF}\, N_1 + \gamma_{IF}\, N_2 \quad (9)$$

N_1 and N_2 are respective ambiguities of L_1 and L_2 according to the station *A* and the satellite *i*.

Step 2: double difference technique

For the GAMIT software, used in this study to retrieve tropospheric parameters (see Herring et al., 2010), the double difference technique allows to remove clock errors from Eq. 8. In fact, considering two GNSS stations (*A* and *B*) and two satellites (*i* and *j*), we can form double differences ($\varphi^{ij}_{AB,IF}$) of the IF combination observations of the Eq. 8:

$$\varphi^{ij}_{AB,IF} = \frac{f_1}{c}\left(D^{ij}_{AB} + T^{ij}_{AB}\right) + N^{ij}_{AB,IF} \quad (10)$$

with the notations

$$*^{ij}_{AB,IF} = \left(*^i_{A,IF} - *^i_{B,IF}\right) - \left(*^j_{A,IF} - *^j_{B,IF}\right) \quad (11)$$

$$*^{ij}_{AB} = \left(*^i_A - *^i_B\right) - \left(*^j_A - *^j_B\right) \quad (12)$$

Step 3: positions and resolution of ambiguity to extract tropospheric error

In practice, to reconstruct information about the troposphere (T^{ij}_{AB}), it is necessary to resolve phase ambiguities ($N^{ij}_{AB,IF}$) and to compute the geometric term (D^{ij}_{AB}). This term can be computed if station *A* and *B* positions are well known.

Step 4: ZTD adjustment by geodetic software and mapping function

Phases measurements (φ) between each couple of stations and each couple of visible satellites are projected in the zenith direction using mapping function (see Fig. 1). Considering the separated tropospheric error (T^{ij}_{AB}) established from double differences of mapped IF combinations ($\varphi^{ij}_{AB,IF}$), geodetic software allow to adjust a precise measurements of ZTD for the network of selected stations.

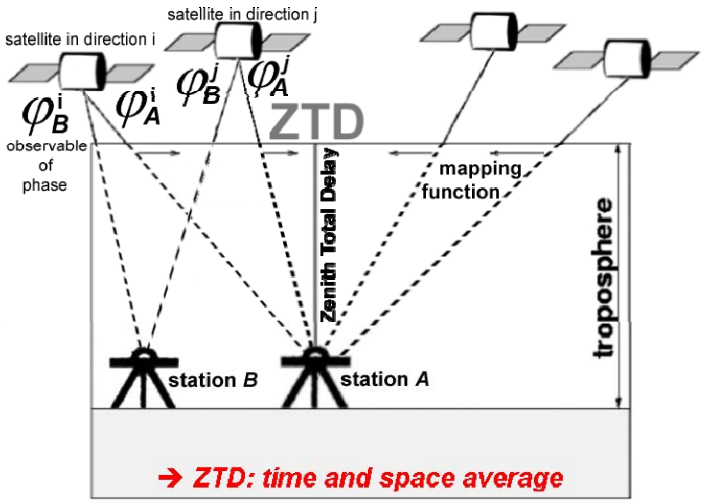

Figure 1. Illustration of the zenith total delay (ZTD) of the neutral atmosphere estimated by geodetic software (a time and space average considering every observables of phases).

For each baseline, an adjustment of the tropospheric error T_{AB}^{ij} is performed, which represents an adjustment of the difference of ZTD between stations *A* and *B*:

$$T_{AB}^{ij} = \left(T_A^i - T_B^i\right) - \left(T_A^j - T_B^j\right) \cong \left(ZTD_A - ZTD_B\right).\left(mf_{sym}(\varepsilon_i) - mf_{sym}(\varepsilon_j)\right) \quad (13)$$

where

$$\begin{aligned} T_A^i &\cong ZTD_A \,.\, mf_{sym}(\varepsilon_i) = L^i{}_{sym,A} \\ T_B^i &\cong ZTD_B \,.\, mf_{sym}(\varepsilon_i) = L^i{}_{sym,B} \\ T_A^j &\cong ZTD_A \,.\, mf_{sym}(\varepsilon_j) = L^j{}_{sym,A} \\ T_B^j &\cong ZTD_B \,.\, mf_{sym}(\varepsilon_j) = L^j{}_{sym,B} \end{aligned} \quad (14)$$

The assessment of mean zenith total delays, for example ZTD_A and ZTD_B at stations *A* and *B*, are processed considering isotropic mapping function (mf_{sym}) of *Niell* (1996) for example (with spherical symmetry) which depends on elevations (for example elevations ε_i and ε_j of satellites *i* and *j*), and the least square adjustments of tropospheric isotropic errors delays in direction of each visible satellites (for example $L^i{}_{sym,A}$, $L^i{}_{sym,B}$, $L^j{}_{sym,A}$ and $L^j{}_{sym,B}$). The final solutions of ZTD assessments adjust constant values for zenith delays according to a defined period (a time-window configured in calculations). To resolve these inversion solutions of ZTD, carrier phase's measurements of all visible satellites ($\varphi_A{}^i, \varphi_B{}^i, \varphi_A{}^j, \varphi_B{}^j, \ldots$) are considered to achieve double differences of the IF combination ($\varphi_{AB,IF}^{ij}, \ldots$) and used in calculations (space average) during a selected time-window (time average). Resolutions of ambiguities and well known positions of stations allow estimations of double differences tropospheric errors terms ($T_{AB}^{ij}, \ldots$) which are linked to the ZTD of each couple of stations for a defined baseline (ZTD_A, ZTD_B,…). Considering *k* epochs of 30 seconds in the defined time-window used by geodetic software adjustments of ZTD (a quarter of hours for example), and considering the number n_j of visible satellites at each epoch *j*, ZTD can be established by:

$$\left| ZTD - \frac{1}{k}\sum_{j=1}^{k}\left(\frac{1}{n_j}\sum_{i=1}^{n_j}\frac{L_{sym}^i(\varepsilon_i)}{mf_{sym}(\varepsilon_i)}\right)\right| < \mu \quad (15)$$

Concretely, ZTD resolved by geodetic software are the results of the minimisation of each μ ($\mu \to 0^+$) obtained during the inversion calculation which adjusts each $L^i{}_{sym}(\varepsilon_i)$. ZTD are

supposed constant during the time-windows chosen to obtain the adjustment. During calculations processes representative zenith tropospheric average corrections (ZTD) can be precisely adjusted for each GNSS sites of the selected network.

2.2 The horizontal delay gradients of the neutral atmosphere

The number of visible satellites and the accuracy of STD reconstructions are critical to identify exactly the location of small-scale tropospheric structures. For this reason, a second tropospheric parameter has been introduced in the least square adjustment of geodetic software: the horizontal delay gradients (*Chen and Herring*, 1997). These are characterised by two components G_{EW} and G_{NS} (respectively east-west and north-south). GNSS gradients represent a correction of phase residuals projections depending on elevations (ε_i) and on azimuths (α_i) of visible satellites (anisotropic contribution). An inclined plane model of troposphere (Fig. 2) schematised by linear thickness and density variations is considered to define horizontal gradients during the adjustments of tropospheric parameters (*Davis et al.*, 1993; *Gradinarsky*, 2002). The correction provided by GNSS gradients possesses its own mapping function (mf_{az}) (*Chen and Herring*, 1997). The formulation of azimuth anisotropic contribution (L^{i}_{az}) to STD reconstruction depends on the satellite direction (elevation and azimuth).

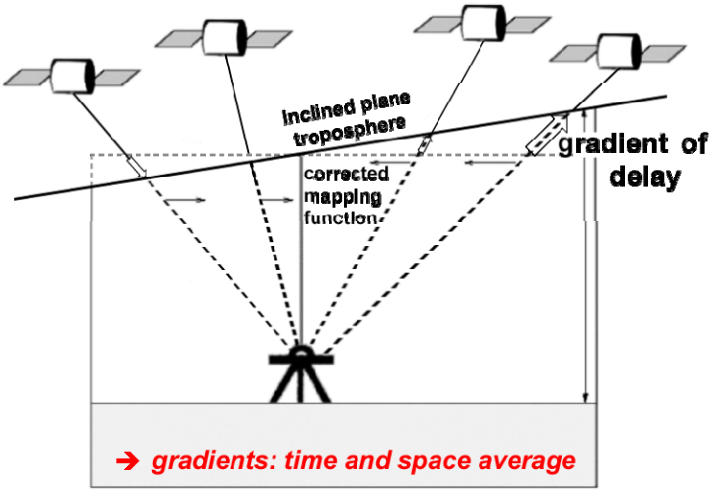

Figure 2. Illustration of horizontal gradients of delays by geodetic software (anisotropic correction of phase observables residuals projected in the zenith direction).

The GNSS horizontal delay gradients are expressed by an equivalent additional distance. The convention of GAMIT geodetic software (*Herring et al.*, 2010) is to resolve GNSS gradient components at 10° of elevation (centimetre values), but using mapping functions measurements of gradients can be converted into the zenith direction (millimetre values). Generally, values of GAMIT gradients components do not exceed 15 cm. Intuitively, a positive value (of 5 cm for example) of G_{EW} represents that the STD at 10° of elevation in the east direction is 5 cm larger than the STD at 10° of elevation in the west direction (a value of STD at 10° of elevation is approximately 14 m at sea level). Usually considering a cutoff angle of 10° in calculations, GNSS gradients concern a conic zone of 50 km around the GNSS site (hypothesis that water vapour density over 10 km is negligible). Considering G_{EW} of 5 cm, ZTD of a site located 25 km eastward at the same altitude is about 9 mm larger, which approximately represents an Integrated Water Vapour content (IWV) about 1.5 kg/m² larger. G_{EW} component (of 5 cm) corresponds to a zenith differential value of about 1.6 mm which can allow imaging ZTD from a network of stations. ZTD and gradients can be resolved every 15 minutes. In the same way than for ZTD, horizontal gradients represent also a time and space average adjustment according to the different visible satellites and phase measurements by ground-based receivers for a defined period.

2.3 The slant total delay of the neutral atmosphere

In the literature, the term T_A^i (Eq. 1, 2 and 3) is called as the slant total delay of the neutral atmosphere (STD). Phase measurements are ambiguous. For this reason, STD can not be directly measured. Using geodetic software, a reconstruction of STD can be established considering three tropospheric parameters: 1) the ZTD (symmetric contribution), 2) the horizontal delay gradients (asymmetric contribution), and 3) the residuals (final adjustment in direction of a defined satellite).

Contribution with spherical symmetry (L_{sym}) to STD

Slant Total Delay (STD) of the neutral atmosphere in direction of each visible satellite, which is the tropospheric error T_A^i presented Eq. 1, is not directly available. The use of the tropospheric model and mapping functions is required to estimate STD. According to ZTD, the isotropic delay (L^i_{sym}) can be restored in direction of satellite *i* with elevation ε_i by:

$$L^i_{sym}(\varepsilon_i) = ZTD \,.\, mf_{sym}(\varepsilon_i) \tag{16}$$

This isotropic contribution to STD is independent of the azimuth α_i of the selected satellite, and can define a cone of path delay around a GNSS site (spherical symmetry).

Contribution with azimuthal asymmetry (L_{az}) to STD

The use of a simple model of inclined plane troposphere allows to resolve the horizontal delay gradients (two components G_{EW} and G_{NS}). The first order of the anisotropic contribution to delays (L^i_{az}) induced by water vapour and eventually hydrometeors (up to 50 km around GNSS site) in direction of satellite *i*, can be formulated depending on elevation ε_i and azimuth α_i of this satellite:

$$L^i_{az}(\alpha_i, \varepsilon_i) = mf_{az}(\varepsilon_i) \,.\, \left(G_{NS} \,.\, \cos(\alpha_i) + G_{EW} \,.\, \sin(\alpha_i)\right) \tag{17}$$

This expression of anisotropic contribution to STD combines a mapping function (mf_{az}, which depends on the elevation ε_i) with gradients components connected to the azimuth α_i (azimuthal asymmetry).

Final reconstruction of STD with residuals

Geodetic softwares (e.g. BERNESE or GAMIT) consider double differences of linear combinations of carrier phases measurements (contained in RINEX data files) to resolve precise positioning solutions and atmospheric parameters (*King*, 1985; *Dong and Bock*, 1989; *Blewitt*, 1989; *Leick*, 1989; *Teunissen et al.*, 1998). The two tropospheric parameters adjusted by geodetic software are ZTD and horizontal gradients. These parameters allow a reconstruction of the STD in direction of a satellite *i* with an elevation ε_i and an azimuth α_i, which is equivalent to the tropospheric error (T_A^i) of a station *A* (see Eq. 1). To detect small scale structure the addition of L^i_{sym} (obtained from ZTD), L^i_{az} (obtained from horizontal gradient components) with L^i_{res} (residuals from the adjustment of ZTD and gradients), allows a precise reconstruction of STD:

$$STD(\alpha_i, \varepsilon_i) = T_A^i = L^i_{sym}(\varepsilon_i) + L^i_{az}(\alpha_i, \varepsilon_i) + L^i_{res}(\alpha_i, \varepsilon_i) \tag{18}$$

The residual observations L^i_{res} is the post-fit phase residuals of the inversion calculation performed by geodetic software, called "*One-Way Postfit Residuals*". This is the third tropospheric parameters available from geodetic software every epoch of 30 seconds in direction of each satellite. Values of L^i_{res} rarely exceed few centimetres. In practice, for some cases these post-fit residuals can not be only due to tropospheric effects. These can contain all remaining unmodeled effects. Using an analysis of the phase centre variation of the antenna of station, non-tropospheric residuals can be avoided. From the meteorological point of view, the final STD reconstruction (with residuals) can be very useful to detect small-scale tropospheric structures.

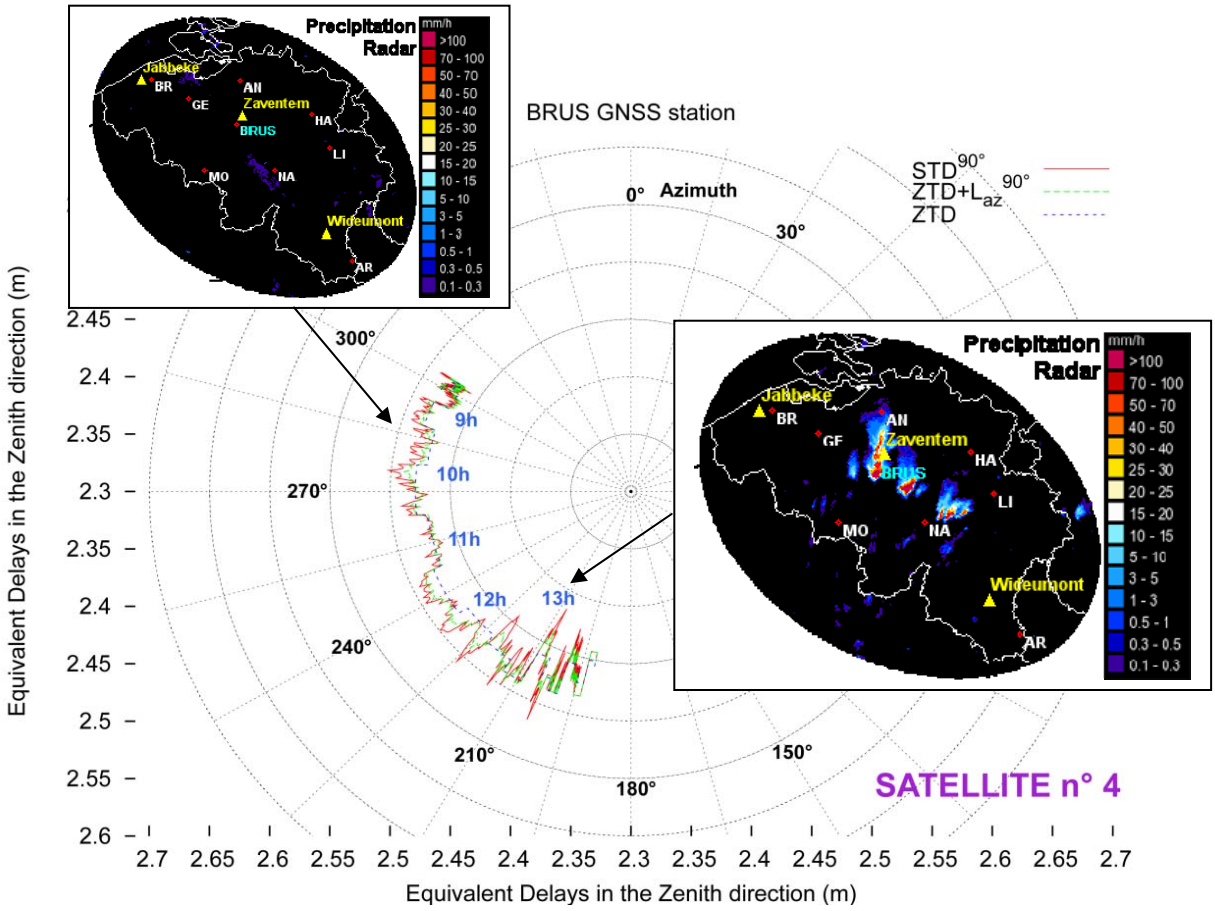

Figure 3. Polar plot of the slant delay in direction of the GPS satellite n°4 measured by BRUS station during the rainfall event 29 June 2005. In red line, the slant delays have been mapped to the zenith direction ($STD^{90°}$). In blue dash line is shown the isotropic contribution to STD (ZTD plot in the azimuthal direction of sat. 4). In green dash line is added the anisotropic contribution of gradients mapped to the zenith ($ZTD+L_{az}^{90°}$). Imaging of precipitation radar at 09:30 and 12:30 UTC are shown

As an example of the potential of STD measurements to identify meteorological activity, Fig. 3 shows the three contributions of the slant delays measured in direction of the GPS satellite n°4. The trajectory of this satellite started at 09:00 UTC north-west of Brussels (azimuth of 300°) and finished at 13:00 UTC south-west of Brussels (azimuth of 195°) on 29 June 2005. In this polar plot, the three contribution of STD (Eq. 18) are mapped in the zenith direction ($STD^{90°} = L_{sym}^{90°} + L_{az}^{90°} + L_{res}^{90°}$; in red line Fig. 3). The isotropic contribution is equal to the ZTD (blue dash line). The anisotropic contribution ($L_{az}^{90°}$) is added to the ZTD (green dash line). We can see at 09:30 UTC that the meteorological situation is quiet (no precipitation on radar image). The slant delays are slightly constant. Strong variations of STD can be observed between 12:00 and 13:00 UTC when the initiation of deep convection took place on the south-west side of Brussels. This shows the interest of STD to identify meteorological structure (blobs of water vapour and convective cells). Brenot et al. (2013) have shown that an indicator of the deep convection can be assessed from ZTD and delay gradients and use for nowcasting. Note that the choice of the network of station is a key parameter to obtain precise measurements of ZTD, gradients and residuals (Brenot et al., 2014). The STD measurements is clearly the best candidate of these three for the NRT detection of meteorological structures.

3 A NEW INDICATOR OF METEOROLOGICAL ACTIVITY

The aim of this section is to find a new indicator of small-scale tropospheric activity showing the evidence of effect in RTK-architecture. Different candidates of tropospheric effects indicators can be considered according to GNSS carrier phase measurements. ZTD and gradients are not the best candidate, being the results of a time and space average (see section 2.1 and 2.2). As shown Fig. 3, reconstructed STDs show a good potential to detect small-scale meteorological structures. The new approach is to consider analysis of time-series of double differences (L_1, L_2) of the IF combination of GNSS phase observations to detect the presence of small-scale structures in the troposphere. The methodology used for this purpose is explained section 2.1. Small-scale structures detected induce disturbances on phase measurements. This study considers stations for which the positions and the geometric distances D_{AB}^{ij} are precisely known. The tropospheric disturbance T_{AB}^{ij} and the ambiguity $N_{AB,IF}^{ij}$ remain the only unknown parameters in the double difference of phase of the IF combination $\varphi_{AB,IF}^{ij}$, as presented Eq. 10. A new observable of phase $\Phi_{AB,IF}^{ij}$ can be estimated:

$$\Phi_{AB,IF}^{ij} = \varphi_{AB,IF}^{ij} - \frac{f_1}{c} D_{AB}^{ij} = \frac{f_1}{c} T_{AB}^{ij} + N_{AB,IF}^{ij} \tag{19}$$

According to Eq. 11, the ambiguity term ($N_{AB,IF}^{ij}$) has the following expression:

$$N_{AB,IF}^{ij} = \left(N_{A,IF}^{i} - N_{B,IF}^{i}\right) - \left(N_{A,IF}^{j} - N_{B,IF}^{j}\right) \tag{20}$$

Ambiguities ($N_{A,IF}^{i}$, $N_{B,IF}^{i}$, $N_{A,IF}^{j}$ and $N_{B,IF}^{j}$) are defined Eq. 9. The phase ambiguity term ($N_{AB,IF}^{ij}$) is a real number with a constant value.

A high content of water vapour and the existence of hydrometeors can induce a strong disturbance of the atmospheric refractivity (*Brenot et al.*, 2006). It can clearly explain sudden variability of tropospheric error T_A^i measured by station *A* for a signal emitted by a satellite *i*. The following expression presents the relation of tropospheric error T_A^i (generally called STD) with neutral atmosphere refractivity (*N*):

$$\text{STD} = T_A^i = 10^{-6} \int N \, ds \tag{21}$$

ds is a differential distance according to path travel of signal between satellite *i* and station *A*. The tropospheric error T_{AB}^{ij} induces the disturbance of the phase observable $\Phi_{AB,IF}^{ij}$ defined Eq. 19 (that represents the double difference of phase of the IF combination with a correction of the geometric distances). This tropospheric error has the following expression:

$$T_{AB}^{ij} = \left(T_A^i - T_B^i\right) - \left(T_A^j - T_B^j\right) \tag{22}$$

The sudden perturbations of the tropospheric errors (T_A^i, T_B^i, T_A^j and T_B^j) by small-scale structures induce direct disturbances of T_{AB}^{ij} and $\Phi_{AB,IF}^{ij}$. Considering two epochs of measurements (epoch t_0 and epoch $t_0 + \Delta t$, for example Δt = 5 min), Fig. 4 illustrates the direct impact of the occurrence of a small-scale tropospheric structure on phase measurements (observables $\Phi_{AB,IF}^{ij}$ and T_{AB}^{ij}).

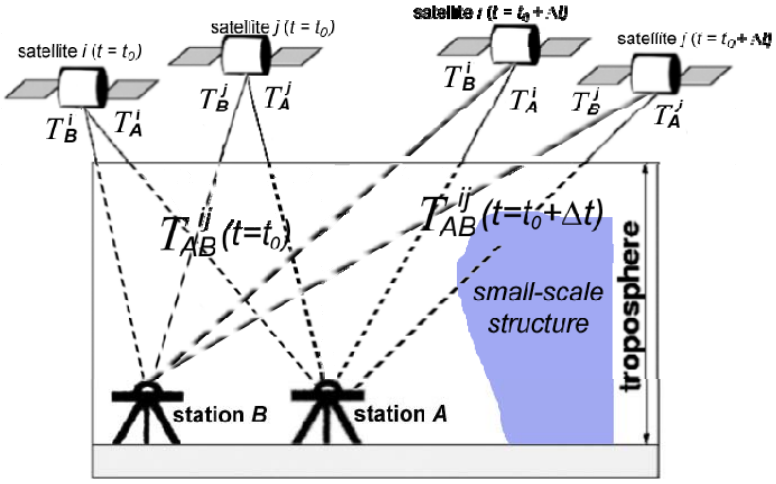

Figure 4. Perturbation of T_{AB}^{ij} induced by a small-scale tropospheric structure for two epochs of measurements (epoch t = t_0 and epoch t = t_0 + Δt).

An RTK-architecture requires the resolution of the ambiguities, nevertheless for this issue all the possible couples of satellites are not considered. For a selected Day Of Year (DOY), reference satellites are chosen to form double differences (DD) and maximise the time periods. The atmospheric scan proceeded by few couples of satellites is sufficient to represent the tropospheric activity. Figure 5 show two examples of tropospheric perturbation T_{AB}^{ij} and ambiguity $N_{AB,IF}^{ij}$ included in the phase observable $\Phi_{AB,IF}^{ij}$ (called IF Double Difference; expressed in cycles) for the 29th of June 2005 (OLLN-NAMR baseline) and the 31st of December 2006 (BRUS-BERT baseline). Without the presence of the troposphere, a constant value of the IF DD should be observed according to the ambiguity $N_{AB,IF}^{ij}$ (which can be a real number). We see clearly the error induced by the troposphere on the IF Double Difference observable ($\Phi_{AB,IF}^{ij}$) time-series presented Fig. 5 (IF DD plots shown by crosses). The impact on IF DD depends on the trajectory of signal through the troposphere (characterised by elevation and azimuth of satellites). In order to display only the influence of small-scale structures, we assess fits of the IF DD time-series with polynomial functions of the 3rd order (dashed lines Fig. 5) and consider the biases between IF DD and the respective fits**,** called IF DD Residuals Fig. 6. The estimation of the bias to the fit removes elevation effects (see Fig. 5 and 6). Small-scale structures are clearly identified for NAMR-OLLN baseline on 29 June 2005 (Fig. 6 between 14:00 and 15:00 UTC). Figure 7 shows a time-series of IF DD Index. To obtain this Index of the tropospheric activity, we convert absolute values of IF DD Residuals (in cycles) to centimetres (multiplying by the wave length: 19.029 cm).

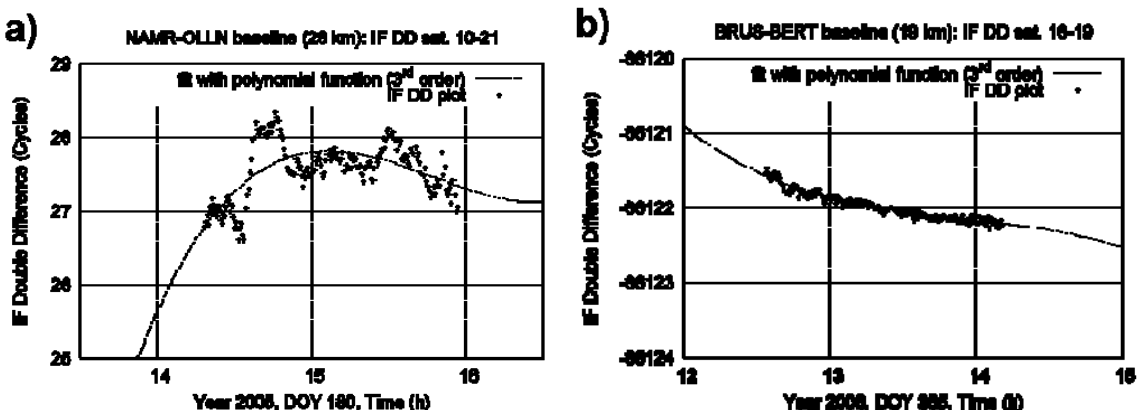

Figure 5. Time-series of IF Double Differences: a) NAMR-OLLN baseline the 29th of June 2005 event (DOY 180), b) BRUS-BERT baseline (no meteorological event on 31 December 2005, DOY 365). The fits of DD time-series with polynomial functions of the 3rd order are shown.

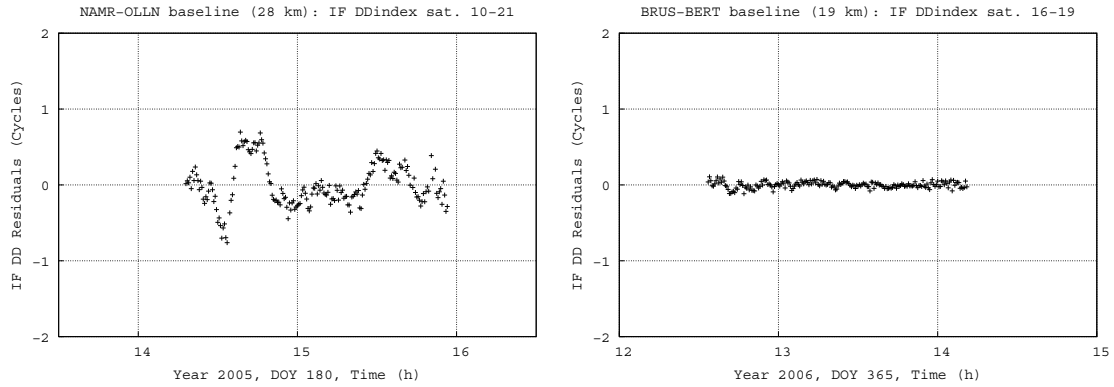

Figure 6. IF DD Residuals time-series of NAMR-OLLN baseline the 29th of June 2005 event (left), BRUS-BERT baseline on the right (no meteorological event on 31 December 2006).

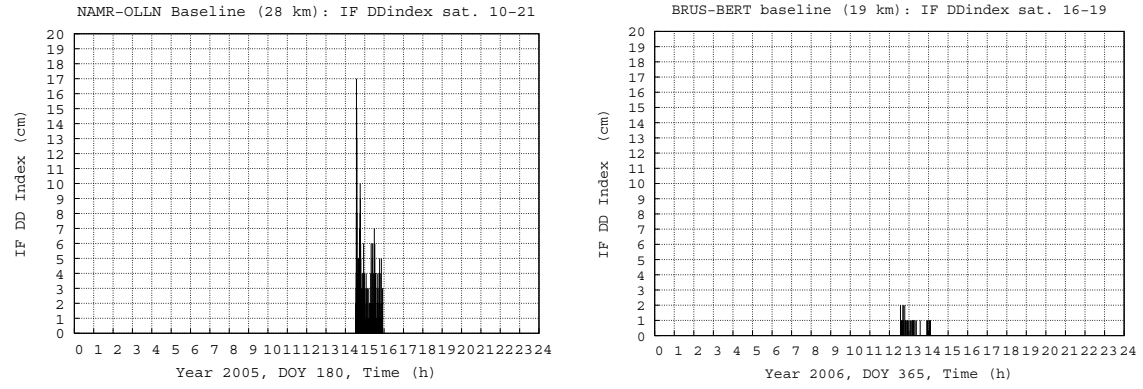

Figure 7. IF DD Index of tropospheric activity of NAMR-OLLN baseline the 29th of June 2005 event (left), BRUS-BERT baseline on right (no meteorological event on 31 December 2006).

According to radar imaging of rain rate (see Fig. 9a), the tropospheric small-scale activity around *Namur* (NAMR and OLLN stations) during DOY 180 of 2005 can be easily observed between 14:00 and 15:00 UTC. Note that a strong tropospheric activity was also observed between 12:00 and 13:00 UTC this day. No tropospheric activity took place around *Brussels* (station BRUS) DOY 365 of 2006 at 13H15 UTC (see Fig. 9b).

Considering all the couples of satellites and available phase measurements for a defined baseline, we can show the daily tropospheric activity (superposition of all the IF DD Index of the selected satellites-stations couples).

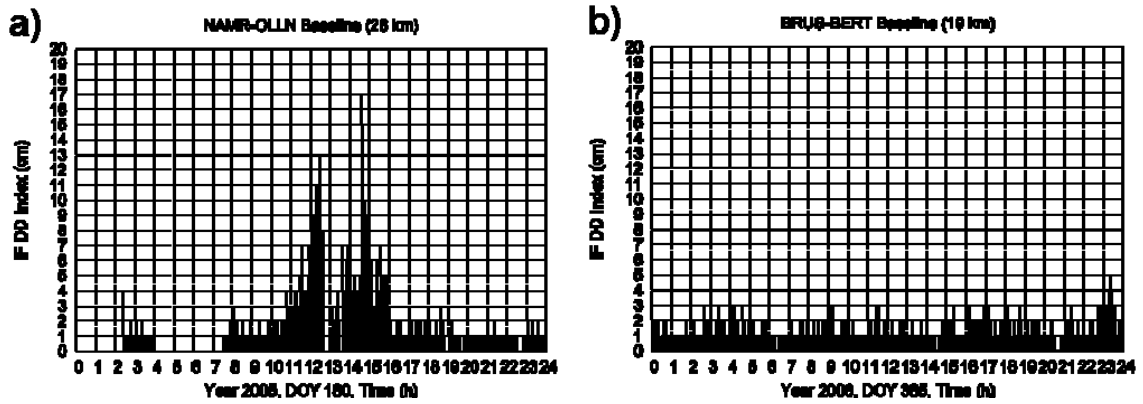

Figure 8. Daily IF DD index of tropospheric activity of a) NAMR-OLLN baseline the 29th of June 2005, b) BRUS-BERT baseline (no meteorological event on 31 December 2006).

Note that on 29 June 2005 no data was available between 00:00 and 02:30 UTC for OLLN station and between 04:00 and 07:30 UTC for NAMR station. In addition, cycle slips have been automatically evicted between 12:30 and 13H30 UTC for the IF DD time-series. This explains the null value of the IFDD Index for some periods shown Fig. 8a for NAMR-OLLN baseline.
Considering every baselines of the Belgian network (baselines from 4 to 30 km, IF DD Index imaging are shown in Fig. 9. The geometric segments (each one corresponding to a baseline) are affected by the maximum IF DD Index estimated at a given moment according to all the couples of satellites considered in our RTK-architecture (at this given moment).

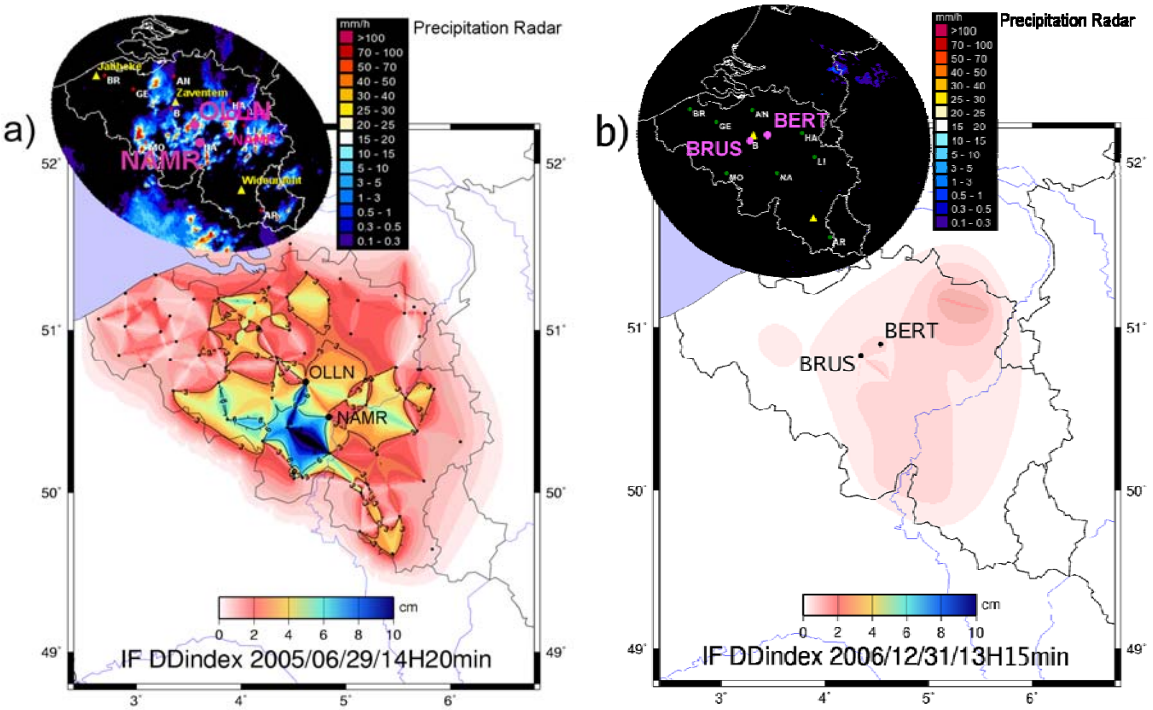

Figure 9. Imaging of the max value of IF DD Index detected in our RTK-architecture and precipitation radar a) 29 June 2005 at 14H30 UTC; b) 31 December 2006 at 13H15 UTC.

White areas presented in Fig. 9 show that no receiver and RINEX data was available or considered. We can see in Fig. 9b that IF DD time-series was slightly affected by tropospheric

activity on the north-west side of Belgium. This meteorological activity is confirmed by radar image with precipitation up to 1 mm/h close to this area. In Fig. 9b, an increased tropospheric activity is observed close to Brussels between 23:00 and 24:00 UTC on 31 December 2006. The radar images show precipitation up to 5 mm/hour 20 km south-west of Brussels.
The IF DD Index imaging (Fig. 9a) is clearly sensitive to sudden perturbation of tropospheric activity. It is sensitive to the occurrence of tropospheric small-scale structures which locally affect couples of satellites emitted signals, and are considered in an RTK-architecture at a given epoch (for more details see Brenot and Warnant, 2008). IF DD Index shows strong disturbances of GNSS signal propagation induced by the troposphere around OLLN station between 14:30 and 15:00 UTC (see Fig. 8a and 9a). The presence of water vapour and hydrometeors above OLLN and on the north-east side of this station affects DD observations for OLLN-NAMR baseline the 29th of June 2005.

4 POSITIONING ERROR DUE TO METEOROLOGICAL ACTIVITY

A part of sources of errors for high accuracy differential GNSS applications comes from the tropospheric delay. Geodetic differential applications are based generally on the assumption that the measurements made by the reference station and by the mobile user (rover) are affected in the same way by the different error sources, in particular by the tropospheric effects (controlled essentially by the water vapour content). Nevertheless, the estimation of NRT positions by differential applications is affected by the spatial and temporal gradient of the tropospheric delay. Small-scale structures in the troposphere are the origin of delay gradients which can degrade the accuracy of differential applications even on distances of a few km. Severe weather conditions can pose a threat for high accuracy GNSS applications. A new indicator of meteorological activity has been introduced in the previous section. To illustrate the interest of this new meteorological indicator for NRT positions, this section shows an example of the related impact on real-time kinematic (RTK) position.
To estimate the influence of meteorological activity and tropospheric structures on RTK positioning, we compute the absolute value of the difference between the “true” station position and the computed position. This absolute value is obtained based on DD corrected for differential ionospheric effects (for more details see Warnant et al., 2008). It is important to underline that this strategy has a disadvantage (eventually residual multipath and measurement noise, bad satellite coverage and geometry, and tropospheric “thickness” effect). For more details see Wautelet et al. (2008).

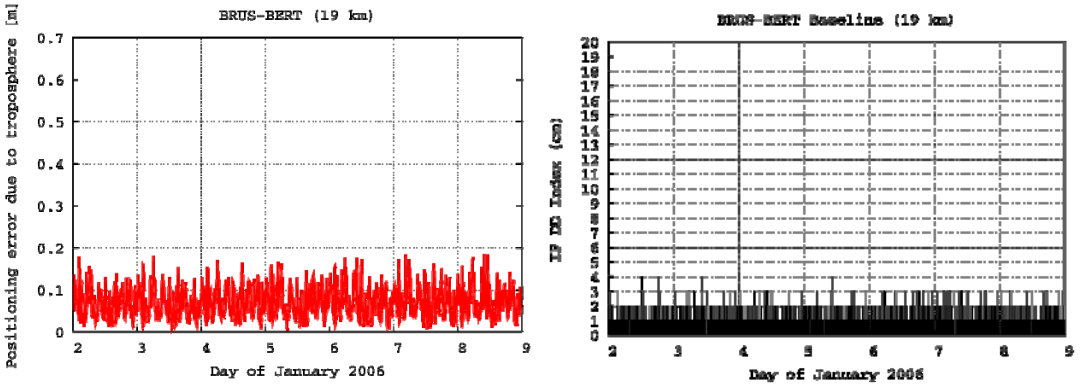

Figure 10. On the left is shown the error on RTK positions expressed in distance (north, east and up components) for BRUS-BERT baseline from 02/01/2006 to 09/01/2006. On the right is shown the corresponding IF DD Index.

To be able to extract the contribution of small-scale tropospheric structures to the positioning error, this error has been tested during quiet and active tropospheric conditions (as measured by our IF DD Index). A strong IF DD Index can be considered for values over 5 (cm). The period of quiet tropospheric conditions (as indicated by our IF DD Index) considered is the month of January 2006. Figure 10 shows that for a baseline of 20 km during quiet condition, the positioning error (distance) due to all error sources (except ionosphere and small-scale structures in

troposphere) ranges from a few centimetres up to about 18 cm. This level of error can be explained by the fact that 20 km is considered as the maximum acceptable baseline length for usual RTK applications. On the other hand, a period with severe weather condition has been studied (rainfall event of the 28th of July 2006). Figure 11 shows positioning errors on distance and IF DD Index for baseline BRUS-BERT observed on 28/07/2006. Even if the background positioning error on this baseline ranges from 5 to 20 cm, the occurrence of IF DD Indexes larger or equal to 5 (of 5+ category) is the origin of increased positioning errors of more than 30 cm. This shows the interest of our IF DD Index in RTK-architecture.

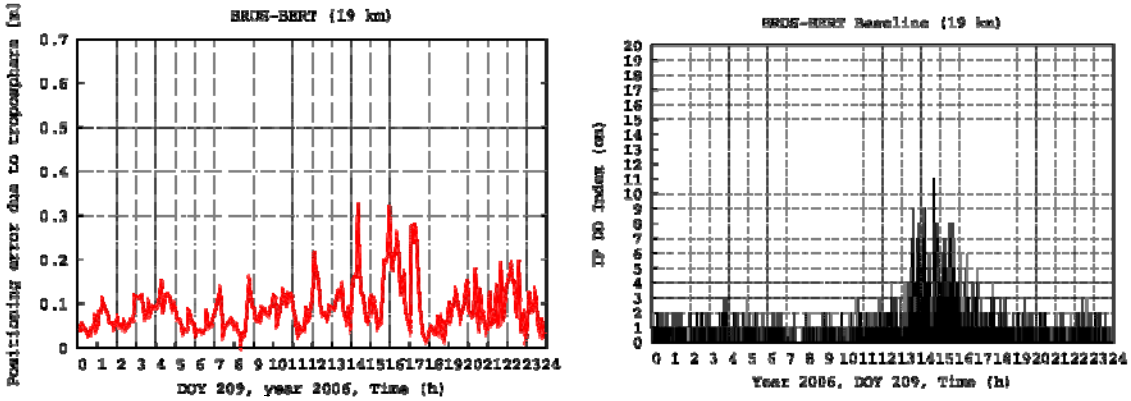

Figure 11. On the left is shown the error on RTK positions expressed in distance (north, east and up components) for BRUS-BERT baseline on DOY 209 of 2006 (heavy rainfall on 28 July 2006). On the right is shown the corresponding IF DD Index.

We proceeded a quantitative study of the positioning error for a range of the period with strong tropospheric activity (Wautelet et al, 2008). We can conclude that IF DD Indexes of 5+ category are the origin of degradations in positioning errors which range between 20 cm and 40 cm even on short baselines (< 20 km). There is a no linear relationship between the magnitude of the IF DD Index and the magnitude of the positioning error (station position computed based on a least square adjustment of all available satellite pairs for the considered period). Nevertheless the number of satellite pairs which are affected by the structures has an important influence on the positioning error (5 satellite pairs affected by an index of 5 bring larger positioning errors than only one satellite pair affected by a large index of 15). Note that for some cases unexplained peaks in the positioning error time series are still observed. Some of them are larger than one metre and have been considered as outliers (these are probably related to unfixed problems in our software). In other cases, we observe smaller peaks certainly due to other problems like bad geometry. Further investigations are necessary to understand the origin of these peaks.

5 CONCLUSIONS AND PERSPECTIVES OF FUTURE APPLICATIONS

This study presents GNSS indicators of meteorological activity that allow the detection of small-scale structures in the neutral atmosphere. The aim is to find a relevant meteorological indicator to warn the impact on NRT positioning solutions (i.e. effect in RTK-architecture for a dense network of stations). The scope of this paper is to present a new NRT index of meteorological activity based on double-difference of the ionosphere-free combination (so called IF DD index). Contrary to ZTD imaging and horizontal delay gradients measurements from geodetic software (result of a mean time and space solution), the IF DD Index imaging is clearly sensitive to sudden disturbance of tropospheric activity. That means sensitive to the occurrence of tropospheric small-scale structures which locally affect couples of satellites emitted signals considered in NRT positioning architecture (e.g. RTK-architecture) at a given epoch. The impact (risk of error) of meteorology on positions is presented for a dense network of station (example NRT GNSS indexes for severe weather conditions in Belgium and the impact on RTK positioning solutions). The contribution of small-scale tropospheric structures (detected using the IF DD Index) to the RTK error budget has been analysed. We found that, in most of studied cases, IF DD Indexes of

5+ category are the origin of degradations in positioning errors which range between 20 cm and 40 cm even on short baselines (less than 5 km). Nevertheless, it appears that, on baselines larger or equal to 20 km, it is not always possible to extract the contribution of small-scale tropospheric structures to the positioning error from the background positioning error (due to other sources as residual multipath, noise, constellation geometry).
In the frame of future collaborations with partners, the use of the IF DD Index can be planed operationally in NRT positioning architecture for dense networks. Further investigations are necessary to understand the origin of some of the remaining positioning errors. The establishment of proper statistical correlation between our activity indexes (troposphere and ionosphere) and the RTK positioning error requires the analysis of larger data sets.
On the other hand, the NRT indicator of tropospheric activity can be very useful for meteorologists and nowcasting. We plan to improve the time and space imaging of the IF DD Index using multi-GNSS satellites in collaboration with forecasters.

REFERENCES

Bevis, M., S. Businger, T. A. Herring, C. Rocken, R. A. Anthes, and R. H. Ware (1992). GPS Meteorology: Remote Sensing of Atmospheric Water Vapor Using the Global Positioning System, *J. Geophys. Res.*, 97 (D14), 15,787-15,801.

Blewitt, G. (1989). Carrier Phase Ambiguity Resolution for the Global Positioning System Applied to Geodetic Baselines up to 2000 km, *J. Geophys. Res.*, 94, 10,187-10,203, 1989.

Boehm, J., B. Werl and H. Schuh (2006). Troposphere mapping functions for GPS and very long baseline interferometry from European Centre for Medium-Range Weather Forecasts operational analysis data., J. Geophys. Res., 111, B02406, doi:10.1029/2005JB003629.

Brenot, H., V. Ducrocq, A. Walpersdorf, C. Champollion and O. Caumont (2006). GPS Zenith Delay Sensitivity evaluated from High-Resolution NWP Simulations of the 8-9th September 2002 Flash-Flood over Southeastern France, *J. Geophys. Res.*, vol. 111, D15105.

Brenot, H. and R. Warnant (2008). Characterization of the tropospheric small-scale activity, Technical Report ESA, WP250, GALOCAD project.

Brenot, H., J. Neméghaire, L. Delobbe, N. Clerbaux, P. De Meutter, A. Deckmyn, A. Delcloo, L. Frappez and M. Van Roozendael (2013). Preliminary signs of the initiation of deep convection by GNSS, Atmos. Chem. Phys., 13, 5425-5449, doi:10.5194/acp-13-5425-2013, 2013.

Brenot, H., A. Walpersdorf, M. Reverdy, J. van Baelen, V. Ducrocq, C. Champollion, F. Masson, E. Doerflinger, P. Collard and P. Giroux (2014). A GPS network for tropospheric tomography in the framework of the Mediterranean hydrometeorological observatory Cévennes-Vivarais (southeastern France), Atmos. Meas. Tech., 7, 553-578, doi:10.5194/amt-7-553-2014.

Chen, G. and T. A. Herring (1997). Effects of atmospheric azimuthal asymmetry on the analysis of space geodetic data, *J. Geophys. Res.*, *102*(B9), 20489–20502.

Davis, J. L., G. Elgered, A. E. Niell and C. E. Kuehn (1993). Groundbased Measurements of Gradients in the _Wet_ Radio Refractivity of air, Radio Science, 28, 1003-1018.

Dong, D.-N. and Y. Bock (1989). Global Positioning System Network Analysis With Phase Ambiguity Resolution Applied to Crustal Deformation Studies in California, *J. Geophys. Res.*, 94, 3949-3966.

Ifadis, I. I. (1986). The Atmospheric Delay of Radio Wave: Modelling the Elevation the Elevation Dependence on a Global Scale, *Technical Report #38L*, Chalmers University of Technology, Göteborg, Sweden.

Gradinarsky, L. P. (2002). Sensing Atmospheric Water Vapor Using Radio Waves, Ph.D. thesis, School of Electrical Engineering, Chalmers University Of Technology, Göteborg, Sweden.

Hajj, G., E. Kursinski, L. Romans, W. Bertiger and S. Leroy (2002). A Technical Description of Atmospheric Sounding by GPS Occultation, *Journal of Atmos. and Solar-Terres. Physics*, 64, 451-469.

Haan, S., J. Jones and H. Vedel (2006). EUMETNET GPS Water Vapour (EGVAP), Presentation at European Meteorological Society, Ljubljana, Slovenia.

Herring, T. A. (1992). Modeling Atmospheric Delays in the Analysis of Space Geodetic Data, Proceedings of the Symposium on Refraction of Transatmospheric Signals in Geodesy, Netherlands Geodetic Commission, *Publications on Geodesy*, Delft, the Netherlands.

Herring, T. A., R. W. King and S. C. McClusky (2010). Documentation for the GAMIT GPS Analysis Software, version 10.4, Tech. rep., Mass. Inst. Tech., Cambridge, USA.

Hopfield, H. S. (1969). Two-Quartic Tropospheric Refractivity Profile for Correcting Satellite Data, *J. Geophys. Res.*, 74, 4487-4499.

King, R. W., E. G. Masters, C. Rizos, A. Stolz and J. Collins (1985). Surveying with GPS, *Monograph 9*, School of Surveying, University of New South Wales, Kensington, Australia.

Leick, A. (1989). GPS Satellite Surveying, *Wiley-Interscience*.

Leick, A. (2004). GPS Satellite Surveying 3rd Edition. *John Wiley & Sons*, New York, 435p..

Marini, J. W. and C. W. Murray (1973). Correction for Laser Range Tracking Data for Atmospheric Refraction at Elevation above 10 Degrees, *Report X-591-73-351*, NASA GSFC, Greenbelt, MD.

Niell, A. E. (1996). Global mapping functions for the atmosphere delay at radio wavelengths, *J. Geophys. Res.*, vol. 101, n°B2, 3227-3246.

Resch, G. M. (1984). Geodetic Refraction, chap. Water Vapor Radiometry in Geodetic Applications, pp. 53-84, *Springer-Verlag*, New York.

Saastamoinen, J. (1972). Atmospheric Correction for the Troposphere and Stratosphere in Radio ranging of satellites, Geophys. Monogr. Ser., 15, 247-251, edited by S. W. Henriksen, et al..

Seeber, G. (2003). Satellite Geodesy Second Edition. *de Gruyter*, New-York, 589 p..

Solheim, F., J. Vivekanandan, R. Ware and C. Rocken (1999). Propagation Delays Induced in GPS Signals by Dry Air, Water Vapor, Hydrometeors, and Other Particulates, *J. Geophys. Res.*, 104 (D4), 9663-9670.

Warnant, R., G. Wautelet, J. Spits and S. Lejeune (2008). Characterization of the ionospheric small-scale activity, Technical Report ESA, WP220, GALOCAD project.

Wautelet, G., S. Lejeune, S. Stankov, H. Brenot, R. Warnant (2008). Effects of small-scale atmospheric activity on precise positioning, Technical Report ESA, WP230, GALOCAD project.

Teunissen, P., A. Kleusberg, Y. Bock, G. Beutler, R. Weber, R. B. Langley, H. van der Marel, G. Blewitt, C. C. Gload and O. L. Colombo (1998). GPS for Geodesy, *Springer*, 2nd Edition.